

## Research Article

### Optimization Inversion of the Ground Stress Field of Bohai Sea and Its Adjacent Area

<sup>1,2</sup>Zongxiang Xiu, <sup>3</sup>Baohua Liu, <sup>1,2</sup>QiuHong Xie, <sup>1,2</sup>Guozhong Han,  
<sup>1,2</sup>Yanpeng Zheng and <sup>1,2</sup>Xishuang Li

<sup>1</sup>First Institute of Oceanography, State Oceanic Administration,

<sup>2</sup>Key Laboratory of Marine Sedimentology and Environmental Geology,

<sup>3</sup>National Deep Sea Center, Qingdao 266061, China

**Abstract:** An optimization inversion model of the ground stress field of Bohai Sea and its adjacent area is established by combining Hooke-Jeeves optimization algorithm and finite element method. The study area was simplified into two 2D sections, a shallow and a deep section, for optimization inversion analysis in consideration of the spatial distribution of the measuring points. The main faults in the study area were simulated by 2D surface to surface contact model, in which the friction state between hanging wall and footwall was modeled by Coulomb friction model. The objective function is established by least squares method, according to the difference values between calculated ground stress data and measured ones. The results show that a plausible ground stress field distribution of Bohai Sea and its adjacent area can be obtained with less data by the optimization inversion method. When there are less measuring points, the optimization inversion result can be easily affected by the distribution of measuring points and the distance of each measuring point to the model boundary; when there are more measuring points, the inversion errors at the checkpoints can be obviously reduced and a more reasonable integrated inversion result can be obtained.

**Keywords:** Bohai sea and its adjacent area, ground stress, Hooke-Jeeves direct search method, least square method, optimization inversion

## INTRODUCTION

Bohai Sea, located in the central part of Bohai Bay Basin, is the relative concentration region of offshore oil and gas development in china, as it is one of the hydrocarbon enrichment areas in Bohai Bay Basin. But meanwhile, the Bohai Sea area has been the most intense area of tectonic activity in East China since the Neogene, with high repetition of strong earthquake (Feng *et al.*, 1988; Lai *et al.*, 2007). Therefore, the ground stress distribution of this area is very complicated. It has been known that the ground stress field has not only important influence on hydrocarbon migration, accumulation and preservation (Zeng *et al.*, 2010; Sun *et al.*, 2008), but also on the oil and gas engineering construction (Chen and Feng, 2006; Kang *et al.*, 2010). To carry out the study of stress distribution of Bohai Sea area can provide useful references for the development of offshore oil and gas of this area.

At present, the ground stress fields obtained by different disciplines or methods may be different, even contradictory (Xu *et al.*, 1999). Although Finite Element Method (FEM) has been considered to be a

fast and effective method for stress field calculation, the boundary condition, loading mode and the initial stress state are usually the difficult problems, because of the complexity and uncertainty of geological structure. A two-dimensional finite element model has been used by Chen *et al.* (2005) for the stress distribution of Bohai Sea area. In this model, the influence of original tectonic stress was neglected; the boundary conditions were applied according to the GPS observation data and the stress field in a large region. The simulation result didn't have absolute meaning and only the change trend of deformation field can be obtained. In other study areas, the boundary load trial-and-error method and boundary load adjustment method were used for ground stress field analysis (Chen *et al.*, 2004, 2002). However, these methods not only have higher requirement for the analysts, but also need huge workloads.

Optimization inversion method, in which the optimization technique and FEM were automatically combined, has been proved to be a convenient and effective method for the stress inversion with less measuring points (Guo *et al.*, 2008). In this method, the objective function can be established by the error function between the simulation results and the

**Corresponding Author:** Zongxiang Xiu, First Institute of Oceanography, State Oceanic Administration, Qingdao 266061, China

This work is licensed under a Creative Commons Attribution 4.0 International License (URL: <http://creativecommons.org/licenses/by/4.0/>).

measured data. The optimal result can be obtained by function with optimization algorithm. The Hooke-Jeeves algorithm (Hooke and Jeeves, 1961), which doesn't need to compute the derivative of objective function, has a simple calculation process and can converge quickly under certain conditions. In view of this, in this study, the Hooke-jeeves optimization algorithm and FEM are combined for the optimization inversion of the ground stress field of Bohai Sea and its adjacent area.

### OPTIMIZATION INVERSION MODEL BASED ON FINITE ELEMENT METHOD

**Regional geological setting:** Bohai Sea is an important part of Bohai Bay Basin which is a typical Mesozoic-Cenozoic fault-depressed basin. Bohai Bay Basin, located in the east block of the North China Craton, is the central region of the destruction of North China Craton. It is bounded by the Tan-Lu fault to the east, Tai-hang fault to the west, Lu-xi uplift to the south and Yan-shan fold zone to the north. As the sea area of Bohai Bay Basin, the tectonic region of Bohai Sea area consists of Bozhong depression and parts of Xia Liaohe depression, Huanghua depression, Jiyang depression and Chengning uplift (Fig. 1). All these tectonic units

approximating the minimum value of the objective are the marine extension of the land part of Bohai Bay Basin, except that Bozhong depression is completely located in the sea area. Considering the integrity of tectonic unit and the unity of tectonic kinematics mechanism, the land parts of Xia Liaohe depression, Huanghua depression, Jiyang depression and Chengning uplift are all included in the model.

As shown in Fig. 1, the simulation area is chosen with the geographic coordinate between 115.6°E-123.6°E and 37°N-41.9°N, in which takes the Tan-Lu fault as the eastern boundary, Cang-dong fault as the western boundary which is the demarcation of Huanghua depression and Cangdong uplift, Luxi uplift as the southern boundary, Yan-shan fold zone and Liaoxi uplift as the northern boundary. The simulation boundaries are simplified as straight lines according to the actual trend.

**Finite element model:** For the inversion calculation of ground stress, a certain amount of measured stress states are needed for the construction of optimization object function. According to the measured data, it can be found that measuring points are mainly distributed in two depth ranges (0~100 m and 2.0~2.5 km). Therefore, the measuring points of different depths are

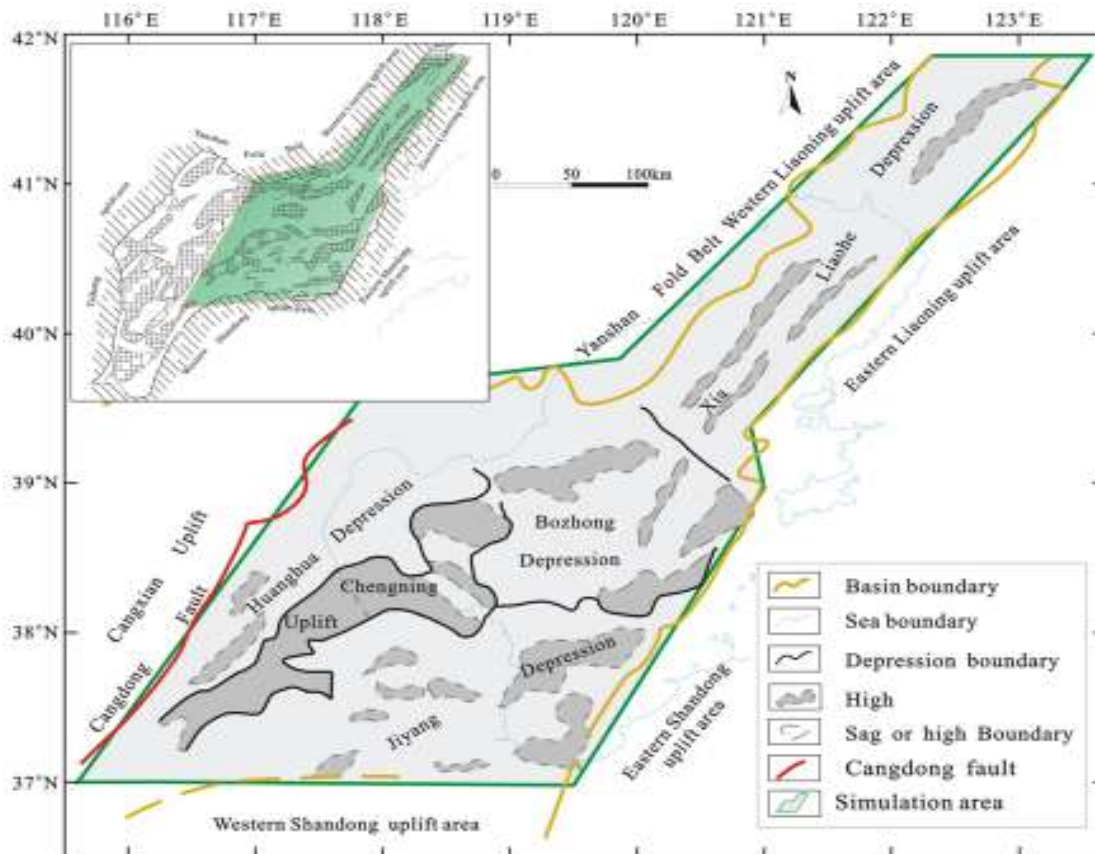


Fig. 1: Finite element simulation area

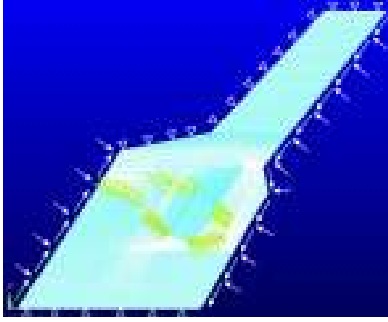


Fig. 2: The FEM model for optimization inversion

projected onto a shallow section and a deep section. A two dimensional FEM model is used for the optimization inversion in this study.

Bohai Bay Basin has been under a push compression action since the Neogene, because of the convergence of Indian plate and Eurasia plate and the subduction of the Pacific Ocean plate underneath the Eurasian plate (Li *et al.*, 2009; Zhang *et al.*, 2004). So, the boundary conditions of the finite element model are simplified as follows: pressure and shear force are applied on the eastern and western boundaries, with the direction of the resultant force are all nearly east-westward; displacement constraints are applied on the southern and northern boundaries, because of the barrier of Liaoxi uplift and Luxi uplift.

As an important factor of having great influence on the ground stress, the main faults in the study area are simulated by the 2D surface-to-surface contact model, in which the Coulomb friction model is used for the contact state of hanging wall and footwall. The 2D plane element with eight nodes is used in the finite element model and there are 37425 elements and 110145 nodes, which are shown in Fig. 2.

**Optimization inversion model:** The optimization inversion process is as follows: firstly, a parameter vector of initial load is preset and the corresponding stress values of the measuring points are calculated by finite element method. According to the optimization algorithm, the parameter vector is changed step by step until the optimization objective function reach the minimum value, which means that the calculated stress values of measuring points approximate well to the measured values. Considering the complexity of optimization inversion of ground stress field, it is still needed to add some constraint conditions in order to make sure the stability and uniqueness of the solution. The ground stress optimization inversion model of Bohai sea area is expressed as follows:

$$\begin{aligned} \text{Find: } & P = \{p_i, i = 1, 2, \dots, n\} \\ \text{Min: } & X(p_1, p_2, \dots, p_n) \end{aligned} \quad (1)$$

$$\text{s.t.: } \underline{p}_i \leq p_i \leq \bar{p}_i$$

where,

P = The unknown boundary load vector

X = The objective function denoted by error function

$\underline{p}_i, \bar{p}_i$  = The upper and lower bounds of the boundary load parameter

At present, the existed data usually only includes the value and direction of the maximum and minimum horizontal principal stress. There are four parameters, denoted by  $\sigma_1^l, \sigma_3^l, d_1^l, d_3^l$  respectively, in the error function. Let  $\sigma_1^c, \sigma_3^c, d_1^c, d_3^c$  be the corresponding parameter values obtained by FEM and then the error function is established by the least square method:

$$\begin{aligned} X(p_1, p_2, \dots, p_n) = \\ \sum_{i=1}^m [a(\sigma_1^l - \sigma_1^c)^2 + b(d_1^l - d_1^c)^2 + a(\sigma_3^l - \sigma_3^c)^2 + b(d_3^l - d_3^c)^2] \end{aligned} \quad (2)$$

where,

$p_1, p_2, \dots, p_n$  = The parameter variables of boundary load

$m$  = The number of measuring points

$a, b$  = The relative weight between the value and direction of horizontal principal stress and their sum equals 1.0

From Eq. (2), it can be found that the error function include two kinds of dimension, which are the stress magnitude and direction. If this function is used,  $a$  and  $b$  must be determined first. However it is hard to find suitable values of  $a$  and  $b$  and they can be easily affected by subjective factors. In view of this, the error function was modified with  $\sigma_x, \sigma_y, \tau_{xy}$ , which can be obtained by converting the measured stress into the model coordinate system. Then the error function can be written as follows:

$$\begin{aligned} X(p_1, p_2, \dots, p_n) = \\ \sum_{i=1}^m [(\sigma_x^l - \sigma_x^c)^2 + (d_y^l - d_y^c)^2 + (\tau_{xy}^l - \tau_{xy}^c)^2] \end{aligned} \quad (3)$$

Based on the proposed optimization inversion idea and method, the optimization variables, pressure and shear forces on the boundaries, are applied in the forms of resultant force and angle. In this study, there are ten variables of pressure values and directions on the eastern boundary and eight variables on the western boundary. The stress data, obtained by in-situ stress measurement, hydraulic fracturing and mathematical regression method, are used for the establishment of error function, according to Eq. (3). The Hooke-Jeeves algorithm is used in this study. The objective function is established according to the measured values of the

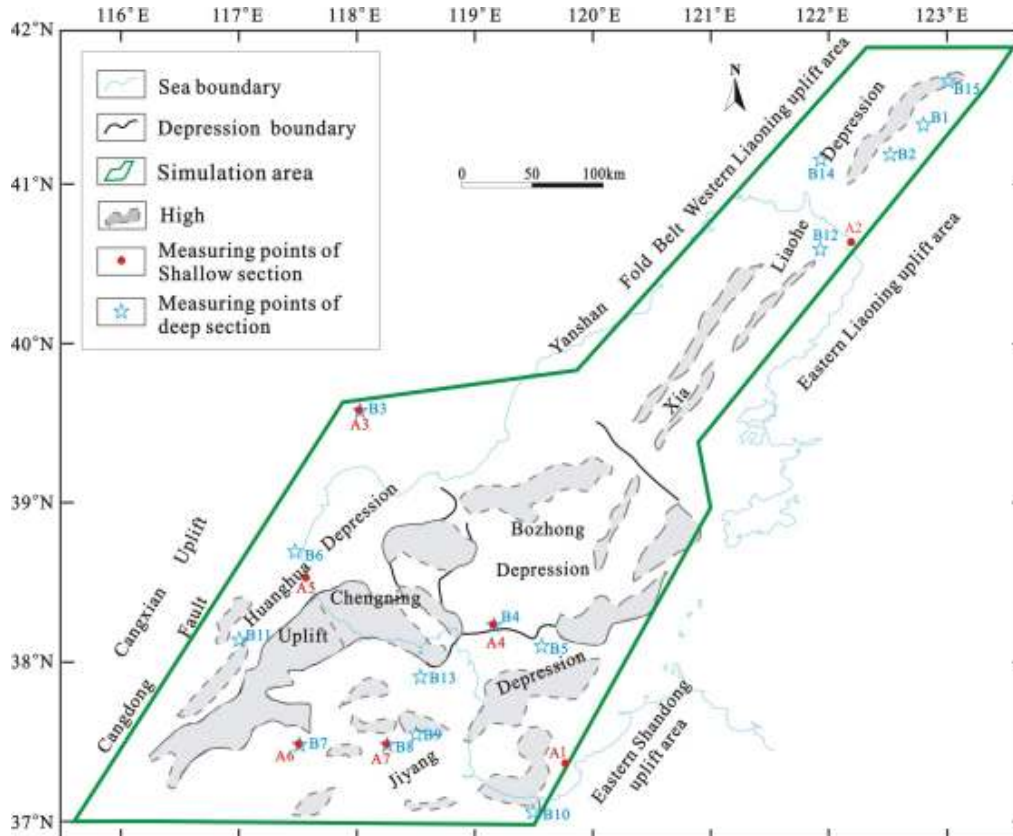


Fig. 3: Distribution of measuring points

measuring points and the corresponding trial calculation results obtained by ANSYS program in batch mode. The whole optimization process is completed by the MATLAB program and in each circulation step, ANSYS would be called in batch mode for the trial calculation. The distribution of measuring points is shown in Fig. 3.

## RESULTS AND DISCUSSION

### Optimization inversion analysis of shallow section:

Table 1 shows the stress data of seven measuring points. In order to verify the optimization inversion results, six points are chosen to establish the objective function and the left one is used as the checkpoint. Considering the influence of measuring point distribution on optimization result, the seven points were arranged to be the checkpoint in turns. Table 1 shows the optimization results and measured stress of shallow section. It can be found that when the point of A7 was chosen as the checkpoint, the minimum errors of optimization inversion results can be obtained. The optimization results of the measuring points involved in optimization process have relatively small errors with the measured values. The maximum errors of the values and directions of the maximum and minimum horizontal principal stress occurred at the point of A2,

which is 5.47 Mpa, 2.97Mpa and 11.05° respectively. This was mainly caused by the boundary effect. For the checkpoint of A7, the corresponding errors are relative small, which is 0.24 Mpa, 0.16 Mpa and 6.53° respectively.

Table 2 shows the relative errors of shallow section under the cases of different checkpoints. It can be found that when the same number of measuring points is used to establish the objective function, their spatial distribution have certain influence on the optimization results. When A1, A2 and A3 are respectively chosen as the checkpoint, the errors at the checkpoints are relatively higher than those of the other four points used as the checkpoints. The maximum error occurs in the case of A2 used as checkpoint. It is considered through analysis that, there are two main reasons for this phenomenon:

- A1, A2 and A3 are relatively close to the model boundary, so the result can be affected by the boundary effect.  
In case A1, A2 and A3, the checkpoint is relatively far from the left six points compared with other cases and because of the limit of algorithm, the farther the checkpoint is from the other points, the lower the optimization inversion precision is.

Table 1: Optimization results and measured stress of shallow section

| Point      | Depth/m | Measured  |             | Optimized |             |
|------------|---------|-----------|-------------|-----------|-------------|
|            |         | Value/MPa | Direction/° | Value/MPa | Direction/° |
| $\sigma_1$ |         |           |             |           |             |
| A1         | 75      | 6.01      | 288         | 5.52      | 279.50      |
| A2         | Surface | 16.60     | 276         | 11.13     | 287.05      |
| A3         | 2.3-5   | 1.60      | 289         | 1.73      | 281.29      |
| A4         | 100     | 2.20      | 85          | 2.37      | 85.62       |
| A5         | 10      | 2.50      | 79          | 2.78      | 77.46       |
| A6         | 5       | 5.65      | 80          | 5.20      | 87.12       |
| A7*        | 5       | 3.87      | 82          | 4.11      | 88.53       |
| $\sigma_3$ |         |           |             |           |             |
| A1         | 75      | 3.81      | 18          | 3.46      | 9.50        |
| A2         | Surface | 10.40     | 6           | 7.43      | 17.05       |
| A3         | 2.3-5   | 1.00      | 19          | 1.09      | 11.29       |
| A4         | 100     | 1.50      | 355         | 1.57      | 355.62      |
| A5         | 10      | 1.50      | 349         | 1.64      | 347.46      |
| A6         | 5       | 3.84      | 350         | 3.65      | 357.12      |
| A7*        | 5       | 2.63      | 352         | 2.79      | 358.53      |

\*: The checkpoint

Table 2: Relative errors of shallow section under the cases of different checkpoints

| Checking point      |              | A1   | A2    | A3   | A4   | A5   | A6   | A7   |
|---------------------|--------------|------|-------|------|------|------|------|------|
| Error of $\sigma_1$ | Value/Mpa    | 0.97 | 2.73  | 0.63 | 0.39 | 0.47 | 0.51 | 0.24 |
|                     | Direction /° | 7.91 | 15.13 | 7.38 | 5.42 | 7.56 | 6.10 | 6.53 |
| Error of $\sigma_3$ | Value/Mpa    | 0.45 | 1.41  | 0.59 | 0.35 | 0.40 | 0.33 | 0.16 |
|                     | Direction /° | 7.91 | 15.13 | 7.38 | 5.42 | 7.56 | 6.10 | 6.53 |

Table 3: Optimization results and measured stress of deep section

| Point | Depth/m   | Measured $\sigma_1$ /Mpa | Measured $\sigma_3$ /Mpa | Measured direction of $\sigma_1$ | Optimized $\sigma_1$ /Mpa | Optimized $\sigma_3$ /Mpa | Optimized direction of $\sigma_1$ |
|-------|-----------|--------------------------|--------------------------|----------------------------------|---------------------------|---------------------------|-----------------------------------|
| B1    | 2250      | 57.40                    | 39.30                    | -                                | 71.5                      | 41.4                      | 84°                               |
| B2*   | 2100      | 96.28                    | 52.41                    | 85°                              | 88.3                      | 47.8                      | 88°                               |
| B3    | 2000      | 57.90                    | 38.65                    | -                                | 64.7                      | 42.6                      | 80°                               |
| B4*   | 2000      | 54.30                    | 35.60                    | 69°                              | 58.6                      | 41.7                      | 71°                               |
| B5    | 2000      | 46.70                    | 36.50                    | 82.5°                            | 53.5                      | 42.1                      | 80°                               |
| B6    | 2268.5    | 64.10                    | 48.80                    | -                                | 67.2                      | 54.3                      | 86°                               |
| B7    | 2172      | 58.30                    | 34.80                    | -                                | 66.5                      | 38.9                      | 89°                               |
| B8    | 2000      | 45.00                    | 34.00                    | -                                | 56.3                      | 39.4                      | 90°                               |
| B9    | 2171      | 57.70                    | 33.70                    | -                                | 65.4                      | 38.5                      | 90°                               |
| B10   | 2379      | 58.80                    | 41.80                    | -                                | 65.8                      | 48.2                      | 75°                               |
| B11   | 1820-2304 | -                        | -                        | 79.5°                            | 55.1                      | 35.6                      | 82°                               |
| B12   | 504-2403  | -                        | -                        | 65°                              | 65.7                      | 43.5                      | 70°                               |
| B13   | 1250      | -                        | -                        | 75°                              | 57.4                      | 35.3                      | 81°                               |
| B14*  | 3000      | -                        | -                        | 96°                              | 79.6                      | 45.7                      | 91°                               |
| B15   | 3000      | -                        | -                        | 70°                              | 52.3                      | 30.2                      | 78°                               |

**Optimization inversion analysis of deep section:** As the same optimization inversion process of shallow section, B2, B4 and B14 are chosen as the checkpoints at the same time, considering the distribution uniformity of measuring points. Limited by the measuring technique, the values and directions of the maximum and minimum horizontal principal stress of some measuring points can't be obtained simultaneously. So, it is the measuring points with stress value and direction or those with only stress value that are used for the establishment of objective function. For the points with only stress direction, they are constrained by state variables with error of  $\pm 10^\circ$ .

Table 3 shows the optimization results and measured stress of deep section. It can be seen that, all errors of the maximum horizontal principal stresses are smaller than 10 Mpa, except for the points of B1 and B8 whose errors are respectively 14.1 and 11.3 Mpa. For the principal stress direction, the errors are all

smaller than  $10^\circ$ . The maximum error of stress value and direction of the three checkpoints is, respectively 7.98 Mpa, 6.1 Mpa and  $5^\circ$ . So it can be consider that the stress values and directions obtained by optimization inversion are close to the measured data.

Figure 4 shows the isoline maps of the maximum horizontal principal stress of deep section. The general trend of distribution of the maximum horizontal principal stress is as follows: stress in the northern part is higher than that in the southern part; the highest stress occurs in Xialiaohe depression, which is in the northern part of the research area, while the lowest occurs in the central part; the stress decreases gradually from the southern part of Xialiaohe depression to Bozhong depression, which shows a relatively low stress in all its area; stress in the land parts of Jiyang depression and Chengning uplift is also somewhat low, but is higher than that in Bozhong depression.

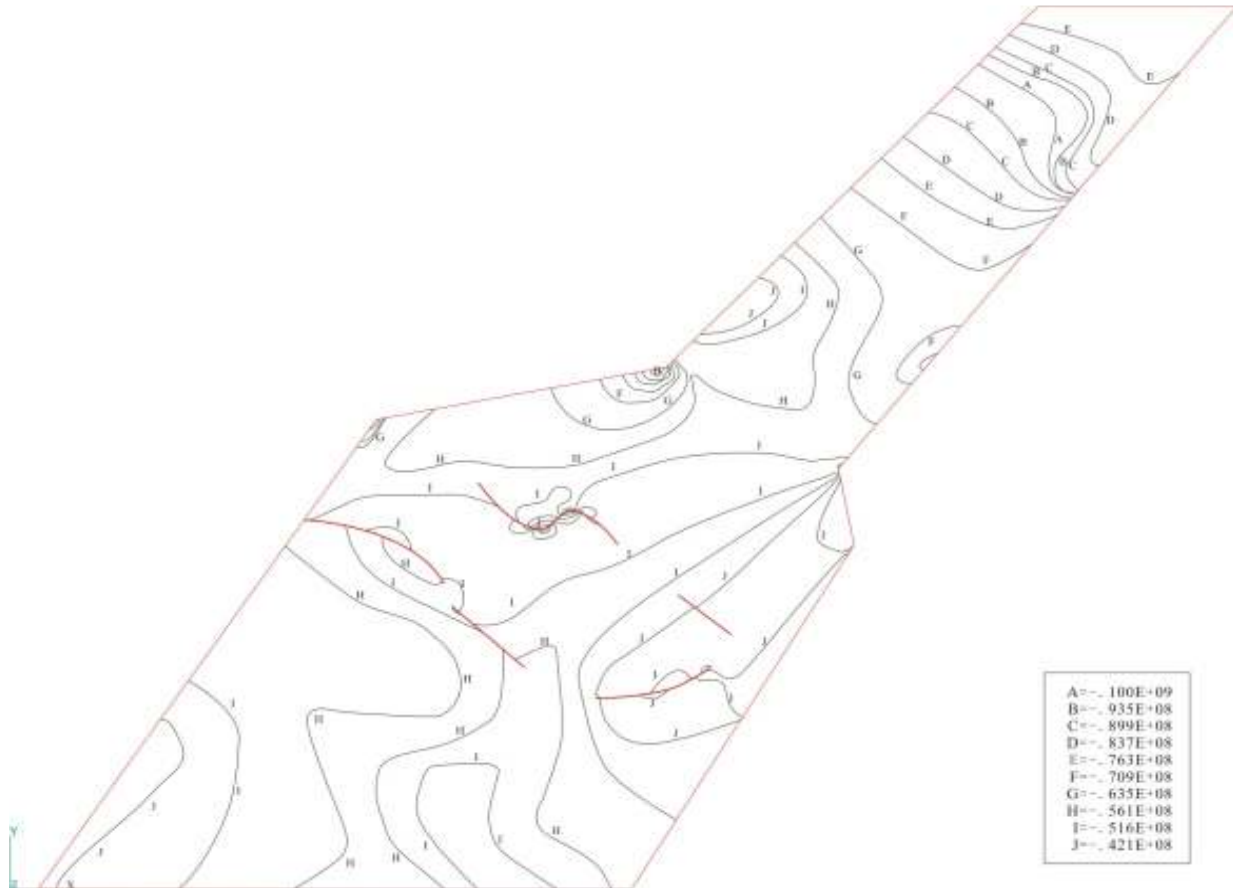


Fig. 4: Isoline maps of maximum horizontal principal stress of deep section



Fig. 5: Direction of horizontal principal stress of deep section

Figure 5 is the direction of horizontal principal stress. From Fig. 5, it can be found that, the direction of maximum horizontal principal stress has obvious zoning characteristics. The horizontal principal stresses in Jiyang depression and the land parts of Chengning uplift and Huanghua depression are mainly compressive stress of E-W and S-N. For Bozhong depression and the marine parts of Chengning uplift and Huanghua depression, it is mainly NE compressive stress and NW tensile stress. The stress distribution of Xiaoliaohe

depression is relatively complicated and the direction of compressive stress is changeable from NNE to EW. The minimum horizontal principal stress is mainly tensile stress, while the compressive stress can still be found near the depression boundary. The direction of maximum compressive stress meets well with that obtained by focal mechanism solution (Dong *et al.*, 1999; Dong and Zhou, 2000) and GPS data (Li *et al.*, 2008; Liu *et al.*, 2006). However, there are still some differences in the direction of the minimum horizontal principal stress, which is mainly affected by the direction of measured stress.

## CONCLUSION

The Hooke-Jeeves direct search method and finite element method are combined for the optimization inversion of the ground stress field of Bohai Sea and its adjacent area. And a plausible stress field can be obtained by this method with few measured data. The method is mainly based on the information of measuring points. When there are less measuring points, the optimization inversion result can be easily affected by the relative spatial positions of measuring point; when there are more measuring points with

reasonable spatial distribution, the inversion errors can be obviously reduced. To improve measuring precision and to increase the number and the coverage of measuring points can improve the calculation precision effectively.

#### ACKNOWLEDGMENT

This study is supported by the National High-Technology Research and Development Program of China (863 Program) under contract No. 2009AA093401, 2010AA09Z302 and the Special Funds for Postdoctoral Innovative Projects of Shandong Province of China under contract No. 201102008.

#### REFERENCES

- Chen, J.T. and X.T. Feng, 2006. True triaxial experimental study on rock with high geostress. *Chinese J. Rock. Mech. Eng.*, 25(8): 1537-1543.
- Chen, X.L., G.G. Chen and H. Ye, 2005. A mathematical simulation for the tectonic stress field of the Bohai sea area. *Seismol. Geol.*, 27(2): 289-297.
- Chen, Z.D., Q.A. Meng, T.F. Wan, Q.J. Jia and T.C. Zhang, 2002. Numerical simulation of tectonic stress field in Gulong depression in Songliao basin using elastic-plastic increment method. *Earth Sci. Front.*, 9(2): 483-491.
- Chen, G.G., J. Xu, Z.J. Ma, Q.D. Deng, J. Zhang and J.M. Zhao, 2004. Recent tectonic stress field and major earthquakes of the Bohai sea basin. *Acta Seism. Sin.*, 17(4): 438-446.
- Dong, X.G., C.Y. Zhou and A.J. Hua, 1999. The analysis on focal mechanism solutions of recent minor earthquakes in pohai straits and its vicinity. *Int. Earthquake*, 13(1): 7-16. Dong, X.G. and C.Y. Zhou, 2000. Circumstance of recent tectonic stress of yanshan-Bohai seismic zone. *S. Chi. J. Seismol*, 20(1): 16-23.
- Feng, D.Y., M. Ichikaywa, H. Matsumoto, J.L. Chen and G.Y. Wu, 1988. A preliminary study on sea-bottom seismograph observation in Bohai Sea area, China. *NW Seismol. R.*, 10(3): 98-122.
- Guo, M.W., C.G. Li, S.L. Wang and G.B. Luan, 2008. Study on inverse analysis of 3-D initial geo-stress field with optimized displacement boundaries. *Rock Soil Mech.*, 29(5): 1269-1274.
- Hooke, R. and T.A. Jeeves, 1961. Direct search solution of numerical and statistical problems. *J. Assoc. Comput. Mach.*, 8(2): 221-229.
- Kang, H.G., J. Lin, X. Zhang and Y.Z. Wu, 2010. In-situ stress measurements and distribution laws in Lu'an underground coal mines. *Rock Soil Mech.*, 31(2): 827-844.
- Lai, X.L., S.L. Li and Y. Sun, 2007. Deep tectonic background of three Ms>7.0 strong earthquakes in Bohai and its adjacent region. *J. Geodesy Geodyn.*, 27(1): 31-33.
- Li, R.S., X.F. Cui, G.L. Diao and H.Y. Zhang, 2008. Temporal and spatial variation of the present crustal stress in Northern part of North China. *Acta Seismol. Sin.*, 30(6): 570-580.
- Li, Y.X., Z.J. Ma, J.H. Zhang, J. Xu and Z.F. Zhang, 2009. Current-day extending motion of Bohai Basin. *Chinese J. Geophys.*, 52(6): 1483-1489.
- Liu, X., R.S. Fu, G.H. Yang, D.P. Sun, Y.H. Dong and Y.P. Han, 2006. Deformation field and tectonic stress field constrained by GPS observations in North China. *J. Geodesy Geodyn.*, 26(3): 33-39.
- Sun, B., L.Y. Shao, W.Z. Li, W.G. Tian and G. Chen, 2008. An analysis of control factors on cbm pooling in daning area, ordos basin. *Nat. Gas Ind.*, 28(3): 40-44.
- Xu, J.S., J.R. Yuan, S.J. Gao, X.A. Lai, Y.X. Li, K.L. Kai and L.Z. Liu, 1999. Research on the present tectonic stress field in north china with GPS observations. *Crus. Deform. Earthquake*, 19(2): 81-89
- Zeng, L.B., H.J. Wang, L. Gong and B.M. Liu, 2010. Impacts of the tectonic stress field on natural gas migration and accumulation: A case study of the Kuqa depression in the Tarim Basin. *Mar. Petrol. Geol.*, 27(7): 1616-1627.
- Zhang, J.H., Y.X. Li, L. Guo and Z.F. Zhang, 2004. Study on present-day deformation and strain field in North China by use of GPS data. *J. Geodesy Geodyn.*, 24(3): 40-46.